

# Electrochemical Study of the Hetero-Bimetallic Complex $[\text{MeNC}(\text{CO})_2\text{Mn}(\text{dppm})_2\text{Pt}(\text{H})(\text{CNMe})]^+ \text{PF}_6^-$ at a Glassy Carbon Electrode

I. S. El-Hallag, A. M. Hassanein, and M. M. Ghoneim\*

Chemistry Department, Faculty of Science, Tanta University, Tanta, Egypt

**Summary.** Cyclic voltammetry (CV), convolution-deconvolution transformation of current, chronopotentiometry (CP), and digital simulation studies were used to evaluate the kinetic parameters of the electrode reaction of the hetero-bimetallic complex  $[\text{MeNC}(\text{CO})_2\text{Mn}(\text{dppm})_2\text{Pt}(\text{H})(\text{CNMe})]^+ \text{PF}_6^-$  in dichloromethane at a glassy carbon electrode (GCE). It was found that the complex undergoes a reduction step at  $-0.895 \pm 0.01$  V and two anodic steps at  $+0.903 \pm 0.01$  V and  $1.370 \pm 0.01$  V. The reduction and oxidation steps are followed by a rapid chemical process. On the basis of the electrochemical results, an overall oxidation process was found to proceed as EEC, while the reduction process proceeds according to an ECEC scheme.

**Keywords.** Cyclic voltammetry; Convolution-deconvolution; Chronopotentiometry; Hetero-bimetallic complex.

## Elektrochemische Untersuchung des hetero-bimetallischen Komplexes

$[\text{MeNC}(\text{CO})_2\text{Mn}(\text{dppm})_2\text{Pt}(\text{H})(\text{CNMe})]^+ \text{PF}_6^-$  mit einer Glaskohlenstoffelektrode

**Zusammenfassung.** Cyclische Voltammetrie (CV), Strom-Konvolution-Dekonvolution, Chronopotentiometrie und digitale Simulation wurden zur Bestimmung der kinetischen Parameter der Reaktion des hetero-bimetallischen Komplexes  $[\text{MeNC}(\text{CO})_2\text{Mn}(\text{dppm})_2\text{Pt}(\text{H})(\text{CNMe})]^+ \text{PF}_6^-$  an einer Glaskohlenstoffelektrode (GCE) in Dichlormethan eingesetzt. Der Komplex zeigt eine Reduktionsstufe bei  $-0.895 \pm 0.01$  V und zwei anodische Stufen bei  $0.903 \pm 0.01$  V und  $1.370 \pm 0.01$  V. Auf die Reduktions- und Oxidationsschritte folgt unmittelbar ein schneller chemischer Prozeß. Aus den elektrochemischen Ergebnissen läßt sich ein Gesamtoxidationsprozeß nach einem EEC – Schema ableiten, während die Reduktion nach einem ECEC – Schema verläuft.

## Introduction

The main advantage that can be expected from the use of convolution procedures in treating CV data is that all available information along the whole *i vs. E* curve is used instead of the peak values alone. The shape of the convoluted and deconvoluted current also provides important information about the nature of the electrode behaviour [1–8]. For example, in the case of fast electron transfer, the convolution

current  $I_1$  of the reverse scan as a function of  $E$  is an exact overlay of that of the forward scan. In the case of fast electron transfer, the deconvolution current ( $dI_1/dt$ ) thus consists of two mirror-image peaks with maximum amplitude  $E^0$  and half-width  $w_p$  equal to  $90.53/n\text{ mV}$  at 298 K, whereas for a quasi-reversible electron transfer the average value of deconvoluted peaks gives  $E^0$ . In the case of a chemical step following the electron transfer (EC), the backward convolution does not return to the initial value, whereas in deconvolution the peak height of the forward scan is greater than the backward one and the difference of height magnitude depends on the rate of the chemical step following the electron transfer [7, 8]. *Saveant et al.* [3, 4] and *Oldham* [5, 6] have proposed the convolution of the current with an inverse square root of time function to produce a transformed variable convoluted current ( $I_1$ ) which is defined as

$$I_1 = \frac{1}{\sqrt{\pi}} \int_0^t \frac{i(u)}{\sqrt{(t-u)}} du \quad 1$$

in Refs. [7, 8]. In the present work, we will use the more complex “kinetic convolution” ( $I_2$ ) expressed as

$$I_2 = \frac{1}{\sqrt{\pi}} \int_0^t \frac{i(u) \cdot \exp(-k_c(t-u))}{\sqrt{(t-u)}} du \quad 2$$

in Refs. [7, 8], where  $I_1(t)$  is the convoluted current at the total elapsed time ( $t$ ),  $i(u)$  is the experimental current at time  $u$ , and  $k_c$  is the homogeneous chemical rate constant. Expression 2 enables the determination of all parameters in an  $\text{EC}_{\text{irrev}}$  reaction [7].

The electrochemistry of organometallic metal–metal bonded complexes has been the object of many studies [9–12]. There has been much interest in the electrochemistry of tertiary phosphine substituted group 6 metal carbonyl complexes [13, 14]. Their investigation should ensure the further development of organometallic electrochemistry [15].

The work described in the present article is concerned with the electrochemical behaviour of the hetero-bimetallic complex  $[\text{MeNC}(\text{CO})_2\text{Mn}(\text{dppm})_2\text{Pt}(\text{H})(\text{CNMe})]^+ \text{PF}_6^-$ , where *dppm* is  $\text{Ph}_2\text{PCH}_2\text{PPh}_2$  (*bis*-(diphenylphosphino)-methane), using various electrochemical methods at a glassy carbon electrode (GCE) as well as digital simulation treatments.

## Results and Discussion

Figure 1a shows an example response of the voltammogram obtained at a sweep rate of 0.2 V/sec at 294 K. In the cathodic direction, the cyclic voltammogram of the  $1 \times 10^{-3} \text{ M}$   $[\text{MeNC}(\text{CO})_2\text{Mn}(\text{dppm})_2\text{Pt}(\text{H})(\text{CNMe})]^+ \text{PF}_6^-$  solution exhibited one reductive peak 1, coupled with an oxidative peak 2 which appears only at sweep rates  $> 0.2 \text{ V/sec}$  (Fig. 1b). The peaks 1 are associated with a small oxidative peak 3. In the anodic direction, the voltammogram revealed two oxidative peaks (4 and 5) within the  $\text{CH}_2\text{Cl}_2/0.1 \text{ M TBAP}$  solvent limit at 294 K and at sweep rates ranging from 0.05 to 0.2 V/sec. The anodic peak 4 is coupled with a cathodic peak 7. A reductive peak 6 coupled with the second oxidative peak 5 appears only at low temperatures.

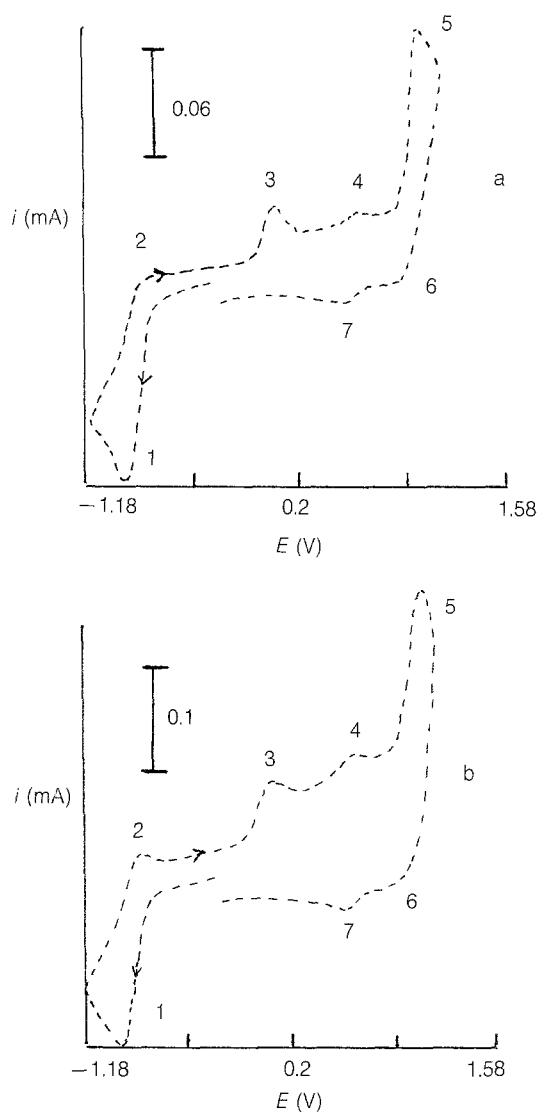


**Fig. 1.** Cyclic voltammogram of the investigated complex in  $\text{CH}_2\text{Cl}_2$  at GCE; 294 K, scan rate 0.2 V/sec (a) and 0.5 V/sec (b)

The oxidative peak 3, combined with the reductive peak 1, is attributed to the oxidation of a chemical product resulting from the reduction of the complex. On scanning the potential in anodic direction, the oxidation peak 3 disappears (Fig. 2), confirming that peak 3 is combined with a reduction process only.

#### *The reduction process*

It has been found that the reduction process of the investigated complex gives a unidirectional single peak (labeled as 1) at 294 K and a low sweep rate (up to 0.2 V/sec) in the sense that there are no coupled reoxidation peaks for this process. The shape and height of the current voltage curves for peak 1 indicate a fast chemical reaction following a quasi-reversible electron transfer [7]. At sweep rates higher than 0.2 V/sec, the oxidation peak 2, coupled with the reduction peak 1 appears (Fig. 1b).

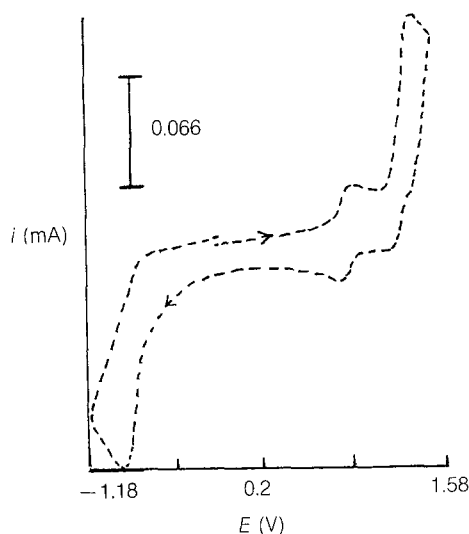


**Fig. 2.** Cyclic voltammogram of the investigated complex on scanning the potential to anodic direction (scan rate 0.2 V/sec, and 294 K)

The small oxidation peak 3 is associated with the reduction peak 1. However, peak 3 is not present when the cathodic potential scan is terminated before the reduction peak 1. The exact location of the oxidation peak 3 varies with the sweep rate. The direction and magnitude of the potential shift is consistent with the lack of a cathodic peak coupled directly to peak 3, confirming the EC oxidation process along peak 3.

The electron transfer for the reduction process was found to be quasi-reversible, indicated by the lack of overlay of the return sweep of the convoluted current on cyclic sweeping (Fig. 3a). The diffusion coefficient ( $D$ ) of the investigated complex was evaluated, after applying background subtraction and correction for uncompensated resistance, from the following relationship [7]:

$$I_{\text{lim}} = nFAD^{1/2}C_{\text{bulk}} \quad 3$$

Here,  $I_{\text{lim}}$  is the limiting value achieved for  $I_1$  when the potential is driven to a sufficiently extreme value past the wave, and the other terms have their usual meanings. The value of the diffusion coefficient was found to be  $2.42 \times 10^{-10} \pm 0.1 \text{ m}^2/\text{sec}$ . The value of the symmetry coefficient  $\alpha$  has been evaluated by the expression 4 [17]:

$$E_p - E_{p/2} = \frac{48}{\alpha_c n_a} \text{ mV at } 25^\circ\text{C} \quad 4$$

The value of  $\alpha_c$  was found to be  $0.39 \pm 0.02$  (Table 2).

The standard heterogeneous rate constant ( $k_s = 4.85 \times 10^{-5} \pm 0.2 \text{ m/sec}$ ) in the case of peaks 2 and 1 as well as for peaks 4 and 7 was evaluated, after applying background subtraction and correction for uncompensated resistance, using the method established by Nicholson [18]:

$$\Psi = \frac{(D_0/D_R)^{\alpha/2} k_s}{[D_0 \pi \nu (nF/RT)]^{1/2}}; \quad 5$$

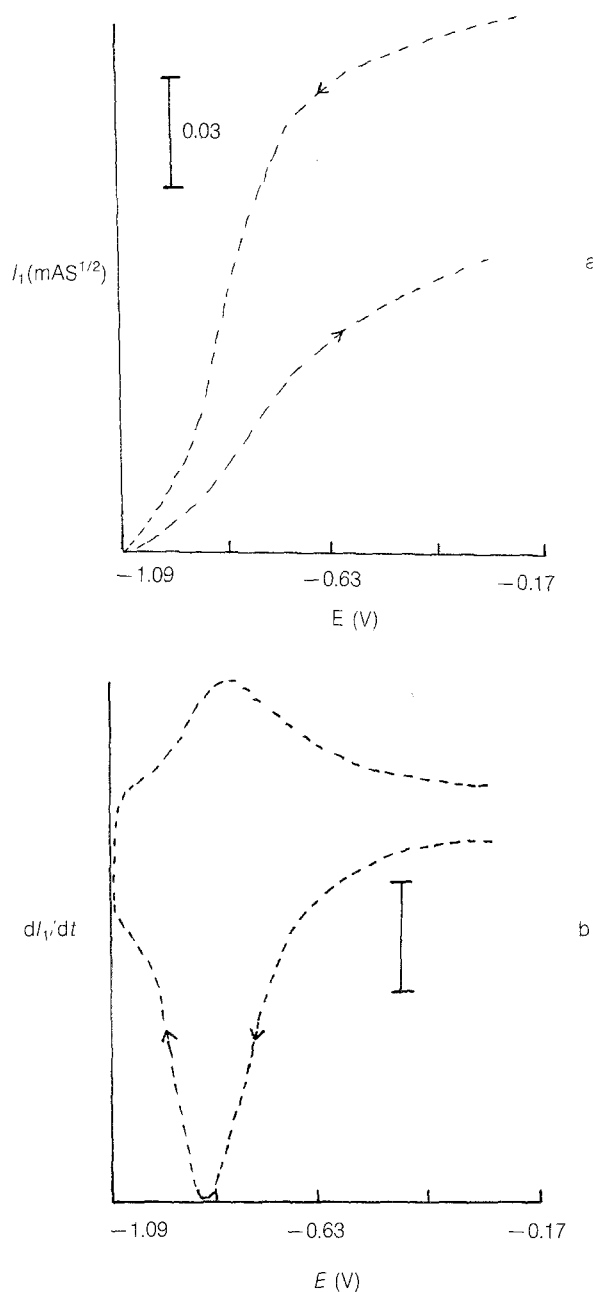


**Fig. 3.** Convolution (a) and deconvolution (b) current of the reduction process (scan rate: 0.2 V/sec)

$\Psi$  is the dimensionless rate parameter; the remaining terms have their usual meanings by determining the variation of  $\Delta E_p$  with  $v$ . Also, in case of peak 5, the standard heterogeneous rate constant ( $k_s = 1.67 \times 10^{-4} \pm 0.2$  m/sec) was determined from the shift of  $E_p$  with  $\log v$  via the following relation [17]:

$$E_p = \frac{\text{const}}{k_s^2} - \frac{2.3RT}{2\alpha n_a F} \log v \quad 6$$

$\alpha$ ,  $D$ , and  $k_s$  were tested and verified from the agreement of experimental and theoretical data via digital simulation using the *Condesim* software by superposition of the simulated voltammograms on the experimental ones (Fig. 4).

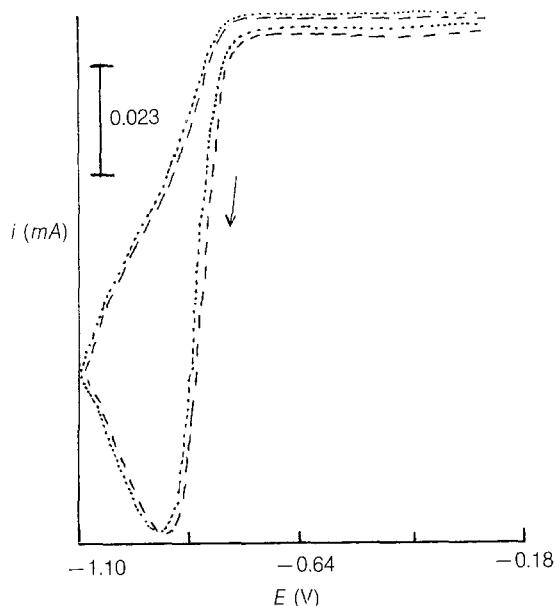


**Fig. 4.** Experimental (---) and theoretical (...) voltammograms of the reduction process (scan rate: 0.2 V/sec)

The  $I_1$  convolution of the reverse scan for the reduction process at all sweep rates (0.05–5 V/sec) does not return to zero current (Fig. 3a), indicating a fast chemical process following the quasi-reversible electron transfer [19, 20].

The deconvolution of the current with the function  $(\pi t)^{-1/2}$  shown in Fig. (3b) gives a significant improvement in the visual presentation of cyclic voltammetric data. The peak displacement of the  $dI_1/dt$  shape (Fig. 3b) provides strong evidence for the quasi-reversible electron transfer process exhibited by the system [20].

According to the relationship 7 [21, 22]

$$I_p = \frac{\alpha n^2 F^2 A v C D^{1/2}}{3.367 R T} \quad 7$$

(where  $I_p$  is the peak height of the forward sweep,  $v$  is the scan rate, and the other terms have their usual meanings), the diffusion coefficient of the complex species under consideration was evaluated from the slope of  $I_p$  vs.  $v$ ; its estimated value is  $2.81 \times 10^{-10} \pm 0.1 \text{ m}^2/\text{sec}$  at 294 K.

The peak width ( $w_p$ ) of the deconvoluted current for a fast electron transfer is equal to  $3.53 R T / n F$ , i.e. 90.6 mV for a fast one electron transfer process. This value depends on the deviation from Nernstian behaviour [22]. ( $w_p$ ) was found to be in the range of 120.6–146.9 mV at a sweep rate of 0.1–0.5 V/sec (Table 1), giving good evidence for the quasi-reversibility of the electron transfer [22].

Peak 3 results from the oxidation of the electroactive product  $P_1$  giving species **D** (Eq. 8). When the potential is switched again to the negative direction after peak 3, the peak coupled directly with peak 3 disappears. The absence of a reductive peak coupled with peak 3 denotes the EC mechanism in which the chemical reaction is too fast on the time scale employed.

From the electrochemical behaviour, the reduction process of the complex under consideration can be viewed as an ECEC system (electron transfer followed by chemical reaction (peaks 1 and 2) and further electron transfer followed by chemical

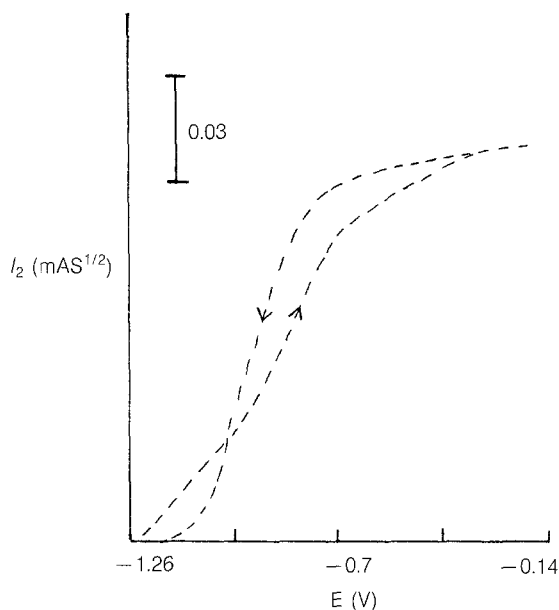
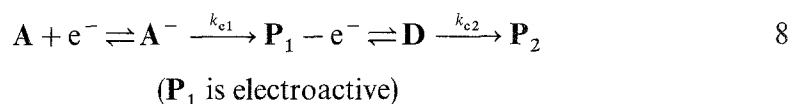


**Fig. 5.** Kinetic convolution ( $I_2$ ) of the reduction process (scan rate: 0.5 V/sec)

reaction (peak 3)).



The  $I_1$  convolution does not adhere to the behaviour expected for a reversible interconversion of the chemical product, and here the nature of the chemical process is unknown.

The homogeneous rate constant ( $k_c$ ) of the chemical step following the charge transfer was determined using equation 2 by fitting the  $k_c$  value. An example of the function  $I_2$ , evaluated with the best-fit value of  $k_c$  (0.85/sec), is shown in Fig. 5.

The diffusion coefficient ( $D = 2.51 \times 10^{-10} \pm 0.1 \text{ m}^2/\text{sec}$ ) of the bulk species determined from cyclic voltammetry data using equation 9 [17] and from convolutive cyclic voltammetry (Eq. 3) was supported by chronopotentiometry, using equation 10 [23].

$$i_p = (2.99 \times 10^5) n(\alpha n_a)^{1/2} A C^{\text{bulk}} D_0 v^{1/2} \quad 9$$

$$I_{\text{lim}} = 2i_c \{t_s/\pi\}^{1/2} = (nFA D^{1/2} C_{\text{bulk}}) \quad 10$$

$i_c$  is the polarization current, and  $t_s$  is the transition time. The value of  $D$  obtained from the chronopotentiometric experiment was  $2.63 \times 10^{-10} \pm 0.1 \text{ m}^2/\text{sec}$ ; this is in good agreement with the result obtained from the CV experiments and the convoluted-deconvoluted current of cyclic voltammetry (Table 2).

#### *The oxidation processes*

The electron transfer of the first oxidative wave (4) was found to be fast. The diffusion coefficient evaluated according to equation 3 was found to be

**Table 1.** Values of peak characteristics extracted from cyclic voltammetry and deconvolution data of the investigated complex at 294 K

$v$ (V/sec)	Reduction (first peak, 1)		Oxidation (second peak, 5)	
	$E_p - E_{p/2}$ (mV)	$w_p$ (mV)	$E_p - E_{p/2}$ (mV)	$w_p$ (mV)
0.1	90.4	120.6	84.2	98.1
0.2	118.5	134.9	95.4	111.4
0.5	150.7	146.9	112.1	126.5
1	180.5	179.3	149.5	141.4
2	210.9	227.2	192.2	164.2

**Table 2.** Values of the electrochemical parameters extracted from cyclic voltammetry (CV), convolution-deconvolution, and chronopotentiometry (CP) data for the investigated complex at 294 K

Parameters	Techniques			
	CV	Convolution	Deconvolution	CP
$k_s$ (m/sec)	$4.85 \times 10^{-5a}$	—	—	—
	$1.66 \times 10^{-3b}$	—	—	—
	$1.67 \times 10^{-4c}$	—	—	—
$D \times 10^{10}$ (m <sup>2</sup> /sec)	2.51 <sup>a</sup>	2.42 <sup>a</sup>	2.81 <sup>a</sup>	2.63 <sup>a</sup>
	2.25 <sup>c</sup>	2.76 <sup>b,c</sup>	2.61 <sup>c</sup>	2.71 <sup>b,c</sup>
$E^0$ , V	-0.895 <sup>a</sup>	—	0.889 <sup>a</sup>	—
	0.903 <sup>b</sup>	—	0.907 <sup>b</sup>	—
	1.370 <sup>c</sup>	—	1.374 <sup>c</sup>	—
$\alpha$	0.39 <sup>a</sup>	—	—	—
	0.42 <sup>c</sup>	—	—	—
$k_c$ (sec)	0.85 <sup>a</sup>	—	—	—

<sup>a</sup> Reduction process (peak 1); <sup>b</sup> first oxidation process (peak 4); <sup>c</sup> second oxidation process (peak 5)

$2.76 \times 10^{-10} \pm 0.1$  m<sup>2</sup>/sec. The  $I_1$  convolution of the second wave (5) does not return to zero indicating a chemical reaction [19]. The value of  $D$  was supported from chronopotentiometry for the oxidative processes using equation 10, and it is found to equal  $2.71 \times 10^{-10} \pm 0.1$  m<sup>2</sup>/sec which agrees well with that evaluated from cyclic voltammetry data and convolution-deconvolution transform (Table 2).

The deconvolution  $dI_1/dt$  of the oxidation process is shown in Fig. 6, revealing the equality and the symmetry of the forward and reverse sweeps of the first oxidation wave (4) in Fig. 1a, whereas the second oxidation wave (5) shows inequality and asymmetry of the forward and backward sweeps confirming the fast electron transfer along first wave and the quasi-reversibility of electron transfer along the



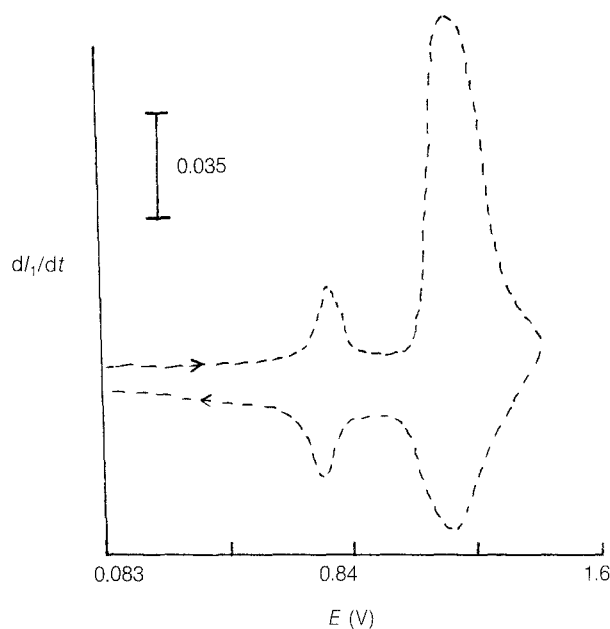


**Fig. 6.** Deconvoluted current of the oxidation process (scan rate: 0.2 V/sec)

second wave. The electrochemical behaviour of the oxidation process can be described as an EEC scheme:



The value of  $E^0$  of wave 4 was calculated at the maximum value of the forward peak due to the alignment of the forward and backward peak at this points, whereas for wave 5 it was calculated from the mean value of the forward and reverse peaks and was found to equal  $0.903 \pm 0.01$  and  $1.374 \pm 0.01$  V, respectively.

The value of the diffusion coefficient ( $2.61 \times 10^{-10} \pm 0.1$  m<sup>2</sup>/sec) was calculated according to the method described by *Alford et al.* (equation 7 [21]). The peak width  $w_p$  of the two waves (labeld 4 and 5) was also used as a tool for testing and supporting the electrochemical behaviour of the complex and it was found to equal  $90 \pm 3$  mV for the first wave, whereas for the second one  $w_p$  depends on the sweep rate, confirming the reversibility and quasi-reversibility of the first and the second electron transfer [22], respectively.

The standard heterogeneous rate constant ( $k_s$ ) of the first oxidation wave was determined experimentally using equation 5 and was found to equal  $1.66 \times 10^{-3} \pm 0.2$  m/sec. From the agreement between the measured voltammogram and the theoretical one, the value of  $k_s$  of the first wave was tested and verified and was found to equal  $1.48 \times 10^{-3} \pm 0.2$  m/sec. Values of  $k_s$  of the second electron transfer and the symmetry coefficient ( $\alpha$ ) were estimated *via* equation 6, and their values were found to be  $1.67 \times 10^{-4} \pm 0.2$  m/sec and  $0.42 \pm 0.02$ , respectively. The data cited in Table 2 indicate that the electrochemical parameters estimated *via* the various equations used in this work are not much different and independent of the method of their determination.

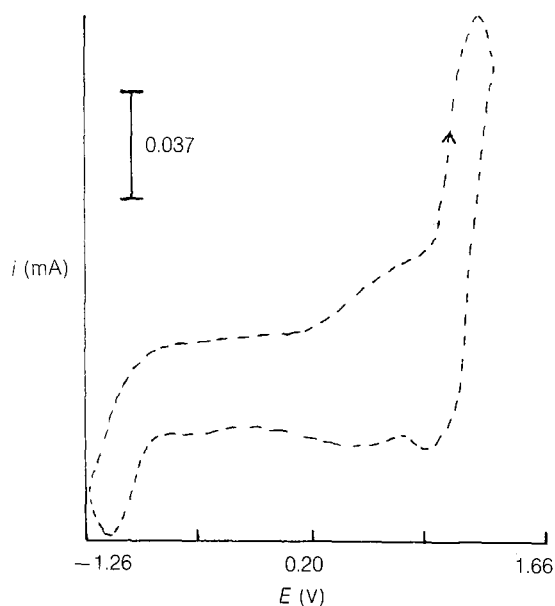


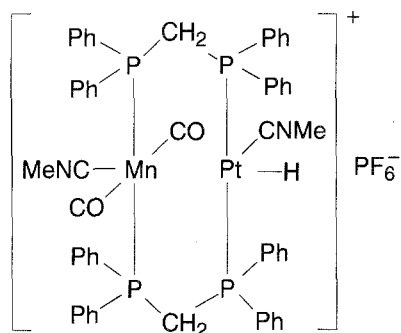
**Fig. 7.** Cyclic voltammogram of the investigated complex (scan rate: 0.5 V/sec, 253 K)

Reducing the temperature to 253 K caused the appearance of the reduction peak 6 coupled with the second oxidation peak 5 and a distortion of the other peaks (Fig. 7), indicating that the rate of the chemical reaction following the electron transfer becomes slow by lowering the temperature [7]. Values of  $E_p - E_{p/2} = 192 \pm 5$  mV and  $\Delta E_p = 384 \pm 5$  mV were obtained for the second anodic peak. The value of  $E^0$  determined from the average value of  $E_{pc}$  and  $E_{pa}$  was found to be  $1.445 \pm 0.01$  V. The temperature effect clearly slows down the chemical reaction following the electron transfer and shifts the reduction potential to a more positive value.

## Experimental

Cyclic voltammetry and chronopotentiometry were performed using a PAR-Potentiostat/Galvanostat model 362 (from EG & G). Electrochemical measurements were made with a glassy carbon electrode in dichloromethane solution using 0.1 M tetrabutylammonium perchlorate as the background electrolyte. The reference electrode used was Ag/AgCl in saturated LiCl-CH<sub>2</sub>Cl<sub>2</sub>. A 1 cm<sup>2</sup> platinum sheet counter electrode was used. Solutions were purged with pure nitrogen before each experiment and an atmosphere of nitrogen was maintained above the working solution during measurements.

Convolution-deconvolution transform and digital simulation of the extracted parameters for the cyclic voltammetric experiments were run on an Amstrad Computer PC 1640 using the *Condecon* and *Condesim* software packages (from EG & G) which allows accurate digital simulation for a wide range of mechanisms for cyclic voltammetry. The investigated hetero-bimetallic (Mn–Pt) dimethyl isocyanide carbonyl complex bridged by Ph<sub>2</sub>PCH<sub>2</sub>PPh<sub>2</sub> ([MeNC(CO)<sub>2</sub>Mn(*dppm*)<sub>2</sub>Pt(H)CNMe]<sup>+</sup>PF<sub>6</sub><sup>−</sup>) was obtained from Prof. B. Shaw at School of Chemistry, Leeds University, United Kingdom. The complex under consideration has the following structure [16]:



Tetrabutyleammonium perchlorate (Polarographic grade) was used as supplied (Fluka G). A fresh stock solution of the investigated complex ( $5 \times 10^{-3} \text{ M}$ ) was prepared in a fresh electrolyte solution ( $0.1 \text{ M TBAP/CH}_2\text{Cl}_2$ ). Cyclic voltammetry experiments were performed at various temperatures between 253 and 294 K.

### Acknowledgements

We thank Prof. Dr. B. Shaw, School of Chemistry, University of Leeds, U.K., for preparation and supplying the investigated complex.

### References

- [1] Whitson PE, Vandeborn HW, Evans DH (1973) *Anal Chem* **45**: 1298
- [2] Oldham KB (1973) *Anal Chem* **45**: 39
- [3] Imbeax JC, Saveant JM (1973) *J Electroanal Chem* **44**: 169
- [4] Saveant JM, Tessier D (1975) *J Electroanal Chem Interfacial Electrochem* **65**: 57
- [5] Oldham KB (1972) *Anal Chem* **44**: 196
- [6] Oldham KB (1983) *J Electroanal Chem* **145**: 9
- [7] Blagg A, Carr SW, Cooper GR, Dobson ID, Gill JB, Goodall DC, Show BL, Taylor N, Bddington T (1985) *J Chem Soc Dalton* 1213
- [8] Dobson ID, Taylor N, Tipping LRH (1986) In: *Electrochemistry, sensors and analysis*. Elsevier, Amsterdam, pp 61–75
- [9] Lemoine P, Giraneau A, Gross M (1976) *Electrochim Acta* **21**: 1
- [10] Miholova D, Vlcek AA (1980) *Inorg Chim Acta* **41**: 119
- [11] de Montauzon D, Poilblance R, Lemoine P, Gross M (1978) *Electrochim Acta* **23**: 1247
- [12] Connelly NG, Geiger WE (1984) *Organomet Chem* **23**: 1
- [13] Bond AM, Carr SW, Colton R (1984) *Inorg Chem* **23**: 2343 and refs therein
- [14] Bond AM, Carr SW, Colton R (1984) *Organometallics* **3**: 541 and refs therein
- [15] Connelly NG (1989) *Chem Soc Rev* **18**: 153
- [16] Carr SW, Shaw BL (1986) *J Chem Soc, Dalton Trans* 1815 and Shaw BL, The University of Leeds, U.K., private communication
- [17] Nicholson RS, Shain I (1964) *Anal Chem* **36**: 706
- [18] Nicholson RS (1965) *Anal Chem* **37**: 1351
- [19] Leddy J, Bard AJ (1985) *J Electroanal Chem* **189**: 203
- [20] IS El-Hallag (1991) Thesis, Tanta Univ, Egypt
- [21] Alford PD, Goto M, Oldham KB (1977) *J Electroanal Chem* **49**: 1390
- [22] Caster DM, Toman JJ, Brown SD (1983) *Anal Chem* **55**: 2143
- [23] Sand HJS (1901) *Phil Mag* **1**: 45

Received January 10, 1995. Accepted (revised) June 19, 1995